bed; h, height of cavity; k, coefficient introduced in (15); p, p_0, pressure inside bed and in cavity; Δp, dimensionless pressure drop; Q, q, dimensional and dimensionless jet flow rates; q_1, q_2, critical values; T, dimensionless height of cavity; T_0, T_1, T_1', T_2, characteristic values of T; **u**, **v**, filtration velocities; u°, u_*, initial filtration velocity in the bed and minimum fluidization velocity; u_0, velocity scale introduced in (14); u^*, velocity scale introduced in (14); u^*, velocity of fictitious flow defined in (15); U, complex velocity; $Z = X + iY$, $z = x + iy$, dimensionless coordinates; $z' = x' + iy'$, dimensional coordinates; α, coefficient of hydraulic resistance; β, parameter from (5); $\Gamma = u_y/u_0$; γ, specific weight of particles' material; ε, porosity; $\zeta = \xi + i\eta$, coordinates in the plane obtained from $z = x + iy$ as a result a of conformal transformation; $\nu = \tan^{-1}\psi^\circ$; ν_m, value of ν giving a minimum of the function G; Φ, φ_f complex and real flow potentials; φ, angle of internal friction; ψ, stream function; ψ°, angle of inclination of boundaries of the region of plastic flow to the vertical.

LITERATURE CITED

1. Yu. A. Buevich and G. A. Minaev, in: Materials of International School on Transfer Processes in Stationary and Fluidized Granular Beds [in Russian], Inst. Teplo- i Massoobmena, Minsk (1977).
2. Yu. A. Buevich, G. A. Minaev, and S. M. Éllengorn, Inzh.-Fiz. Zh., 30, 197 (1976).
3. M. Leva, Fluidization, No. 4, McGraw-Hill, New York (1959).
4. S. S. Zabrodskii, Hydrodynamics and Heat Transfer in a Fluidized (Boiling) Bed [in Russian], Gosénergoizdat, Moscow–Leningrad (1963).
5. L. A. Madonna and R. F. Lama, Ind. Eng. Chem., 52, 169 (1960).
6. N. I. Gel'perin, V. G. Ainshtein, É. N. Gel'perin, and S. D. L'vova, Khim. Tekhnol. Topl. Masel, No. 8, 51 (1960).
7. A. P. Baskakov and A. A. Pomortseva, Khim. Promst. (Moscow), No. 11, 860 (1970).
8. Yu. A. Buevich and S. M. Éllengorn, Inzh.-Fiz. Zh., 34, 221 (1978).
9. A. E. Gorshtein and I. P. Mukhlenov, Zh. Prikl. Khim., 37, 1887 (1964).
10. Yu. A. Buevich, N. A. Kolesnikova, and G. A. Minaev, Inzh.-Fiz. Zh., 33, 586 (1977).
11. M. A. Buevich and S. M. Éllengorn, Inzh.-Fiz. Zh., 37, No. 3 (1979).
12. M. A. Lavrent'ev and B. V. Shabat, Methods of the Theory of Functions of a Complex Variable [in Russian], Fizmatgiz, Moscow (1958).

ANALYSIS OF THE PARAMETERS OF DISCRETE PARTICLE MOTION IN AXISYMMETRIC TURBULENT IMPINGING JETS

V. I. Korobko, I. N. Malyi, L. N. Makarenko, V. K. Shashmin, and L. F. Bulgakova

UDC 532.529

The parameters of discrete particle motion in axisymmetric turbulent impinging air jets are determined.

The method of impinging jets is used extensively at the present time [1] to intensify the heat and mass transfer in technological processes and apparatus. Impinging air jets are quite efficient even for the preparation of concrete mixtures [2]. The self-similar section of sand and cement particle acceleration with a quadratic drag law starting from the plane of the impinging jet is governing in the jet agitation of a concrete mixture. Because of the elastic strain of the air flux at sites of shock merger of the jet, and in the presence of inertial forces, the sand and cement particles from one jet penetrate into an other and are decelerated. These particles do not succeed in being accelerated in the opposite direction since coaxiality of the nozzle sources is spoiled in the subsequent times because of the structural peculiarities of the continuous operation mixer for the preparation of concrete mixtures [2].

Novopolotskii Polytechnic Institute. Translated from Inzhenerno-Fizicheskii Zhurnal, Vol. 37, No. 5, pp. 813-817, November, 1979. Original article submitted January 29, 1979.

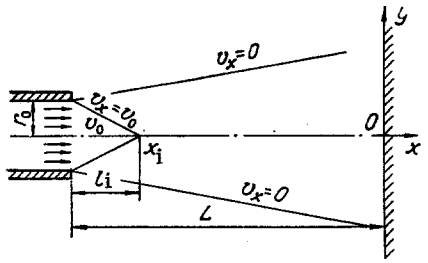

Fig. 1

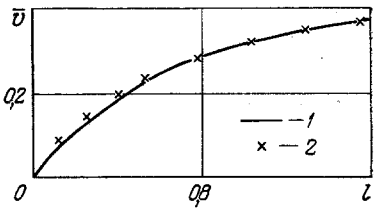

Fig. 2

Fig. 1. Flow diagram.

Fig. 2. Velocity distribution $\bar{v}$ of a discrete aluminum particle in the length l of the deceleration section in impinging flows: 1) computation; 2) experiment [1].

The assumption was made in [1] in a numerical analysis of the process that the velocity of the heat carrier remains constant over the whole track of particle motion, where its magnitude does not exceed 30 m/sec, with the exception of the plane of the jet impingement, where it is zero. Flow deceleration does not occur by a jump in fast impinging flows, but in a zone whose extent is 2-2.5 calibers of the pipeline output section measured from the plane of the impinging jet [3].

It has been established in [1] that the intraphasal exchange in impinging jets is also intensified because of inertial effects since a particle of dense phase in impinging jets is under the continuous action of a sign-varying acceleration. Here the magnitude of the inertial force depends on the value of the velocity gradient dv_1/dx [4], which is two orders of magnitude higher in fast impinging flows than in slow ones. Thus, in an analysis of the process in slow impinging flows [1], the maximum value of the velocity gradient from all the modes investigated is $dv_1/dx \sim 15\ \text{sec}^{-1}$ ($v_0 = 24.6$ m/sec, $L = 1.6$ m) while $dv_1/dx \sim 1600\ \text{sec}^{-1}$ ($v_0 = 240$ m/sec, $L = 0.15$ m) for a concrete mixer [2], e.g., for the process in fast flows. This indicates that the inertial force must be taken into account in the equations of motion of a discrete particle in fast impinging flows during acceleration or deceleration of the flow.

A numerical computation of the motion parameters of discrete particles in axisymmetric turbulent impinging jets is performed in this paper by the method of impinging jets for fast flows.

The problem of the collision of two impinging jets can be considered as the problem of the direct impact of a jet in an infinite plane ($x = 0$, Fig. 1). The air jet issuing from the nozzle can be considered approximately as a free turbulent jet and as diminishing its velocity according to the law of a jet impinging on a plane near the decelerating plane.

Let us consider a jet escaping from a nozzle. There is a constant velocity core near the nozzle exit, i.e., the jet velocity here equals the escape velocity ($v_x = v_0$, Fig. 1). On the basis of computed and experimental data [4], the length of the initial section of the axisymmetric submerged jet equals $\bar{l} = l_1/r_0 \approx 10$. The law of variation of the jet axial velocity is represented as follows [5]:

$$0.22(\bar{x} - \bar{x}_i) = 2.73\left(\frac{1}{\bar{v}_1} - 1\right). \tag{1}$$

Since the spacing between the nozzles equals 2L (Fig. 1), we write an explicit expression for the axial velocity of the submerged air jet:

$$\bar{v}_1 = 1 \quad \text{at} \quad -\frac{L}{r_0} \leqslant \bar{x} \leqslant -\bar{x}_i, \tag{2}$$

$$\bar{v}_1 = [0.08(\bar{x} - \bar{x}_i) + 1]^{-1} \quad \text{at} \quad -\bar{x}_i \leqslant \bar{x} \leqslant 0. \tag{3}$$

The axial jet velocity should first change as in a free jet during motion from the nozzle, and then according to the law of a jet impinging on a plane near the collision plane. Hence, we represent the velocity on the axis of the impinging jets in the form [5]

$$\bar{v}_1 = f(\bar{x})\,[0.08\,(\bar{x} - \bar{x}\,)]^{-1},$$
$$f(\bar{x}) = 1 + \frac{a}{\bar{x}+\alpha} + \frac{b}{(\bar{x}+\alpha)^2} \qquad (4)$$

($a = 2.616$; $b = -1.152$; $\alpha = -3$).

The dimensionless coefficients a, b, α were selected from the following conditions: a) $f(\bar{x}) = 0$ for $\bar{x} = 0$, i.e., it is required that the jet decelerate to zero velocity on the collison plane; b) $d\bar{v}_1/d\bar{x} = -0.8$ for $\bar{x} = 0$, i.e., the velocity curve $\bar{v}_1(\bar{x})$ should approach zero for $\bar{x} = 0$ with the same angular coefficient as for an axisymmetric jet impacting on a plane); c) the jet velocity should tend to the velocity of a free turbulent jet with distance from the collision plane.

Therefore, (4) yields a law of the velocity behavior along the axis of axisymmetric impinging jets.

The equation of steady motion of a spherical particle along the axis of axisymmetric impinging jets in a moving coordinate system is invariantly coupled to the particle in the dimensionless form:

$$\bar{v}\,\frac{d\bar{v}}{d\bar{x}} = \frac{2\rho_1}{\rho+\rho_1}\left\{\frac{3}{8}\,\frac{r_0}{d}\,|\bar{v}-\bar{v}_1|\,(\bar{v}-\bar{v}_1) + (\bar{v}_1 - \frac{1}{2}\,\bar{v})\,\frac{d\bar{v}_1}{d\bar{x}}\right\}. \qquad (5)$$

This equation is obtained from the Chen equation [4], which is written in the moving coordinates [$d/dt = V_1(d/dx)$]. In contrast to [4], the quadratic dependence of the drag force on the velocity according to [1] is taken in the first term on the right. The drag force is here directed opposite to the motion if the solid particle leads the flow, and along the motion if the particle lags behind the flow. It is also assumed that $c_x = 0.5$. The second term on the right determines the inertial force during acceleration or deceleration of the flow. The magnitude of this term is quite essential for the process in fast impinging flows, as we have already mentioned. The axial velocity is $v_1 = v_0$ [formula (2)] to the end of the initial section of the jet ($x = x_i$) when the jet emerges from the nozzle, and the velocity v_1 diminishes according to the law described by (4) during further motion to the plane of jet impingement. Having been given the values of the initial parameters, we integrate (5) numerically in the range $-x_i \leqslant x \leqslant 0$ (Fig. 1) by the Runge–Kutta method of fourth-order accuracy on an M-220M electronic computer.

The results of a computation and measurement [1] of the velocity distribution $\bar{v} = v/v_0$ of a discrete aluminum particle (ρ = 2970 kg/m^3, d = 2.25 mm, Re = 1760) along the length $\bar{l}$ of the deceleration section in slow impinging flows (v = 21.7 m/sec, v_0 = 11.8 m/sec) are compared in Fig. 2.

The computation of 60 variants of discrete sand and cement particle motions in fast impinging air jets (v_0 = 240 m/sec) was performed for a constant density ρ_1 = 2.33 kg/m^3 and the following parameters: sand density ρ_s = 2650 kg/m^3; cement density ρ_c = 3200 mg/m^3; sand diameter d_s = 1, 2 mm; cement particle diameter d_c = 0.005, 0.035, 0.06 mm; dimensionless initial velocity of sand and cement particle insertion into the jet v_i = 0.01, 0.1, 0.3, 0.5; location of the particle insertion $\bar{x}_0 = x/L$ = −0.85, −0.44, −0.15; and r_0 = 4 mm.

The dynamic characteristics of sand and cement particles of different coarseness with a different initial velocity of insertion and different initial location of particle insertion along the jet axis are represented in Fig. 3a and b. The change in jet velocity near the collision plane is superposed here (dashed curve). It is seen from Fig. 3a that the sand particles on being accelerated at the beginning of the motion alter their velocity slightly later by just diminishing it somewhat near the jet collision plane, and that the greater the particle dimater (i.e., its weight), the more it is accelerated to lower velocities. As the initial velocity of sand particle insertion into the jet increases (curves 5-8), its velocity is almost unchanged and depends slightly on the particle diameter, i.e., a sand particle possessing high inertia will react weakly to retardation of the air jet. The farther the particle of sand from the nozzle upon incidence into the jet, the lower the velocity to which it succeeds in being accelerated, since the jet velocity is slowed down.

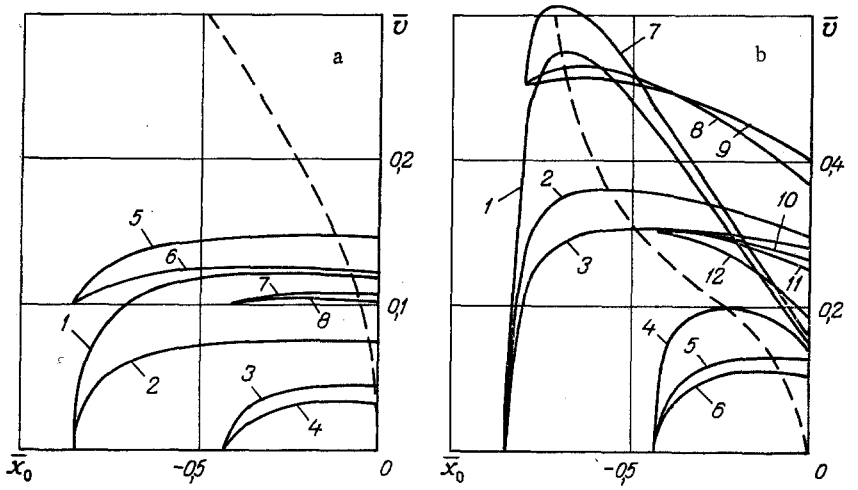

Fig. 3. Change in sand (a) and cement (b) particle velocity along the axis of impinging jets for different coarseness: a) 1, 3, 5, 7) d_s = 1 mm; 2, 4, 6, 8) d_s = 2 mm; b) 1, 4, 7, 10) d_c = 0.005 mm; 2, 5, 8, 11) d_c = 0.035 mm; 3, 6, 9, 12) d_c = 0.06 mm.

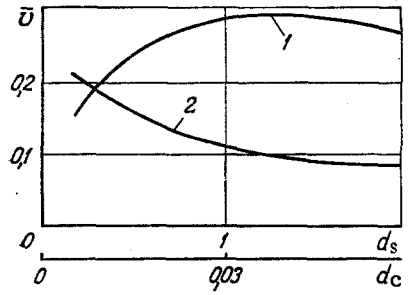

Fig. 4. Velocity of sand and cement particles of different coarseness in the jet collision plane for $\bar{x}_0$ = − 0.85, $\bar{v}_i$ = 0: 1) cement; 2) sand. d_s, d_c in mm.

In is seen from Fig. 3b that the cement particles are accelerated more rapidly, reach the maximal jet velocity, and are decelerated under the effect of the decelerating air jet. Cement particles possessing small diameter (i.e., weight), and, consequently, also low inertia as compared to the sand particles, react rapidly to the change in jet velocity, and the greater the particle diameter (weight), the more weakly does a cement particle react to a change in jet velocity. The farther from the nozzle the cement particle is inserted into the jet, the lower the velocity to which it is accelerated. As the initial velocity of cement particle insertion (curves 7-9, 10-12) increases the more noticeable is the particle inertia: The heavier the particle, the more weakly does it react to a change in the jet velocity.

The dependence of the sand and cement particle velocity in the jet impingement plane on the coarseness of the particles is shown in Fig. 4. If the collision velocity for the sand drops monotonically with the increase in the particle diameter, then for cement a velocity rise in the collision plane is observed at the beginning, and only for d > 0.03 mm does the velocity diminish somewhat. The relative frontal collision velocity (2v) of the particles does not exceed $0.6 \cdot v_0$ = 144 m/sec.

The jet mixing examined permits the preparation of concrete mixtures of given technological parameters because of the high mixing rates as contrasted to existing methods of preparing concrete mixtures [6].

NOTATION

x, y, coordinates (Fig. 1); v_x, jet velocity; v_0, maximum jet velocity; r_0, nozzle radius; l_i, length of the initial jet section; L, spacing between the nozzle and the collision plane; $\bar{x}$, dimensionless coordinate referred to the nozzle radius; $\bar{x}_i$, dimensionless

length of the initial section referred to the nozzle radius; d, particle diameter; ρ_1, jet density; ρ, particle density; c_x, particle drag coefficient; v, particle velocity; v_1, axial jet velocity; ν, kinematic coefficient of the flow viscosity; $\bar{x}_0$, dimensionless coordinate referred to the distance L; d_c, cement particle diameter; d_s, sand particle diameter; $\bar{v}_i$, dimensionless velocity of particle insertion into the jet, referred to v_0.

LITERATURE CITED

1. I. T. El'perin, V. L. Mel'tser, L. L. Pavlovskii, and Yu. P. Enyakin, Transfer Processes in Impinging Jets [in Russian], Nauka i Tekhnika, Minsk (1972).
2. K. M. Korolev, I. N. Malyi, et al., Izv. Vyssh. Uchebn. Zaved., Stroit. Arkhitekh., No. 6 (1973).
3. L. M. Milne-Thompson, Theoretical Hydromechanics, Crane Russak (1976).
4. J. O. Hinze, Turbulence, McGraw-Hill (1975).
5. G. N. Abramovich, Applied Gas Dynamics [in Russian], Nauka Moscow (1976).
6. K. M. Korolev, Intensification of Concrete Mixture Preparations [in Russian], Stroizdat, Moscow (1976).

VELOCITY FIELD IN A LOW-TURBULENCE HYDRODYNAMIC FACILITY, USING A LASER-DOPPLER TECHNIQUE

V. P. Ivanov, V. V. Babenko, V. A. Blokhin, L. F. Kozlov, and V. I. Korobov

UDC 532.526-621.378

This paper describes a laser-Doppler measurement instrument, and also the technique and the results of an investigation of the velocity field obtained with this instrument in the working section of a hydrodynamic facility.

A low-turbulence hydrodynamic facility is designed for the study of physical processes occurring in the boundary layer. In particular, the facility allows one to model various flow regimes, to study the turbulence generation processes, and the physical features in transition of a laminar flow to turbulence, both on rigid surfaces and on elastically damping surfaces [1]. By analyzing available methods for measuring velocity fields in the boundary layer of water flows [2], one can form the following conclusions. The tellurium method is quite simple, economical, and reliable, and also allows one to visualize physical features of the phenomenon studied. It has been used in the low-turbulence hydrodynamic facility to carry out a large number of experiments studying stability of the laminar boundary layer [1]. However, this method has limited capability. For example, for flow velocities greater than 0.2 m/sec it loses information. Although the hydrogen bubble method allows one to enlarge the range of measured velocities, it does not have sufficient accuracy. The track method is extremely laborious. The thermoanemometer has high requirements for purity of the water and temperature stability of the working substance, and in addition, the presence of the sensors in the flow can have an appreciable influence on the results of the investigation, particularly in the study of transition processes. The laser-Doppler velocity meter (LDVM) overcomes a number of these defects, since it is a probeless method, does not require calibration, and is not sensitive to flow temperature fluctuations. The LDVM has high spatial resolution and a linear relation between the flow velocity and the Doppler signal frequency over the entire range of measured velocities.

On the basis of some experience in using the LDVM [3-5], we decided to improve the equipment for processing the Doppler signal. To do this we developed and fabricated an electronic digital analysis system which increases the accuracy of the measurements and yields data on the "instantaneous" velocity.

Institute for Hydromechanics, Academy of Sciences of the Ukrainian SSR, Kiev.

Translated from Inzhenerno-Fizicheskii Zhurnal, Vol. 37, No. 5, pp. 818-824, November, 1979. Original article submitted March 1, 1979.